

TEST OF MODERN THEORETICAL APPROACHES USING MODERN EXPERIMENTAL METHODS*

V.Z. GOLDBERG, G.V. ROGACHEV, R.E. TRIBBLE

Cyclotron Institute, Texas A&M University, College Station, TX, USA

(Received December 2, 2013)

Resonance scattering induced by rare isotope beams provides new possibilities for testing *ab initio* nuclear structure calculations. We discuss such tests involving resonance reactions populating ^{14}F and ^8B levels.

DOI:10.5506/APhysPolB.45.309

PACS numbers: 21.10.-k, 24.30.-v, 25.60.-t

1. Introduction

One of the main goals of modern nuclear theory is to combine nuclear reaction and nuclear structure to provide a unified framework that allows the calculation of level spectroscopy and reaction cross sections starting from nucleon–nucleon and three-nucleon forces. Several theoretical approaches have been suggested (No-Core Large Basis Shell Model (NCSM) [1], Variational Monte Carlo (VMC), and Greens Function Monte Carlo (GFMC) [2], and others) to advance this goal. In these approaches, comparison of the calculations with experiment enables the parameters of the N – N interaction which cannot be properly fixed from the N – N scattering (for example, having a large orbital momentum between nucleons) to be improved and to understand the importance of three-(four) body forces in nuclei.

Recently, the *ab initio* calculations were developed to include descriptions of new phenomena, an example of these was the no-core shell model combined with the resonating-group method (NCSM/RGM) [3]. The very attractive feature of these developments is that the excitation functions for the resonance reactions, such as elastic and inelastic nucleon scattering, (p, n) and (p, γ) reactions, *etc.*, can, in principle, be calculated directly starting from the bare nucleon interaction and compared to the experimental data.

* Presented at the XXXIII Mazurian Lakes Conference on Physics, Piaski, Poland, September 1–7, 2013.

The *ab initio* calculations are difficult and time consuming; therefore, the specific nuclear objects for the analysis are subjected to a careful selection. At present, (1) the calculations are possible for mainly light nuclei ($A < 16$) due to computer time restrictions; (2) to fix the $N-N$ interaction and to provide a path to $2s-1d$ nuclei, nuclei with high isospin are evidently preferable, and (3) it is expected that first predictions for the resonance structure [3] will be more accurate for the lowest excited levels. All the above considerations lead to a study of drip-line nuclei.

For comparison with the untested predictions of the *ab initio* calculations, studies involving rare beams were made. These were the first observation of the ^{14}F [4] nucleus with its lowest states, and a search for predicted, but never observed, low lying levels in ^8B [5, 6]. First experiment provided for a test of calculations for a nucleus with an unusual proton/neutron ratio, the second one provided for a test of the predictions for low lying levels in a light nucleus and the first test for the NCSM/RGM predictions of resonant phase behavior.

2. First observation of ^{14}F

All nuclei near ^{14}F are unstable and most of them (such as $^{15,16}\text{F}$, $^{15,16}\text{Ne}$) are unbound, therefore reaction choices to reach ^{14}F are limited. As a result, there was no experimental information on ^{14}F before work [4]. The most promising way to reach ^{14}F is using a rare isotope beam of ^{13}O which decays by positron emission with the lifetime of 8.6 ms. The ^{13}O nucleus is also far from stability. Since there is no reaction with high cross section to produce ^{13}O from stable isotopes and because the life time is so short, application of the ISOLDE approach (accumulations of rare species with subsequent reacceleration) is not practical. However, an ^{13}O beam can be produced by the $^{14}\text{N}(p, 2n)$ reaction ($Q = -29.1$ MeV) using in-flight separation method.

The 31 MeV/ u beam of ^{13}O with intensity of 5×10^3 p/s was obtained with the facilities of the Cyclotron Institute at Texas A&M University, which include a superconducting cyclotron with primary beam of ^{14}N at 38 MeV/ u with intensity of about 70 pA , a cooled hydrogen gas target with a pressure of 3 atm, and a mass separator, MARS [7]. The low intensity of the secondary beam greatly restricts the choice of possible reactions and methods, however a thick target inverse kinematics (TTIK) measurement [8] can still be applied to measure the excitation function for $^{13}\text{O} + p$ elastic scattering. In the TTIK method, a beam of heavy ions is stopped in the target material and the light recoil product of the elastic scattering reaction (protons in our case) comes out of the target due to the much smaller specific energy loss and is detected. This method allows the measurement of a continuous excitation function from the initial energy down to the lowest detectable energy in a single run. However, there is a rule of thumb restricting the maxi-

mum energy (and correspondingly the number of channels contributing to background processes) to ~ 10 MeV/ u in cases where energies of ~ 1 MeV in the center-of-mass system are of interest. Hence, to apply the TTIK method for the ^{14}F study, the energy of the available ^{13}O beam should be substantially decreased. The experimental approach to the problem was to tag each particle of the beam before and after a degrader which slowed down the beam ions up to ~ 10 MeV/ A . Figure 1 illustrates the experimental setup to accept the 31 MeV/ u ^{13}O beam after MARS separation. The beam was slowed down after MARS, close to the entrance to the scattering chamber, to minimize the loss of intensity. The scattering chamber was filled with methane gas (CH_4) which was used as a safe substitute for hydrogen. A windowless ionization chamber (ICE) was placed in the scattering chamber close to the entrance window (see Fig. 1) to measure the specific energy loss of incoming ions. A pair of quadrant-silicon detector telescopes (QSDs) was also mounted inside smaller windowless ionization chambers. Each QSD consisted of four square detectors ($12.5 \times 12.5 \times 1$ mm 3) and was followed by a similar veto detector to eliminate high-energy particles that punched through the first QSD.

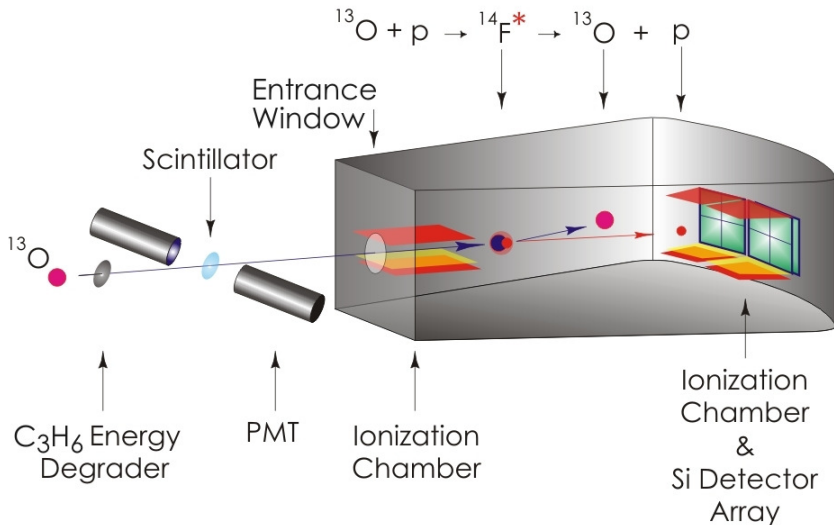


Fig. 1. The setup for the ^{14}F experiment. The “gray box” is the scattering chamber.

Figure 2 shows the excitation functions for $^{13}\text{O} + p$ elastic scattering. Excitation functions were analyzed using the R-matrix approach. The experimental excitation functions in all the Fig. 2 spectra are similar (as could be expected because the spin values involved are small). The stability of the experimental results is important to illustrate the reliability of the data

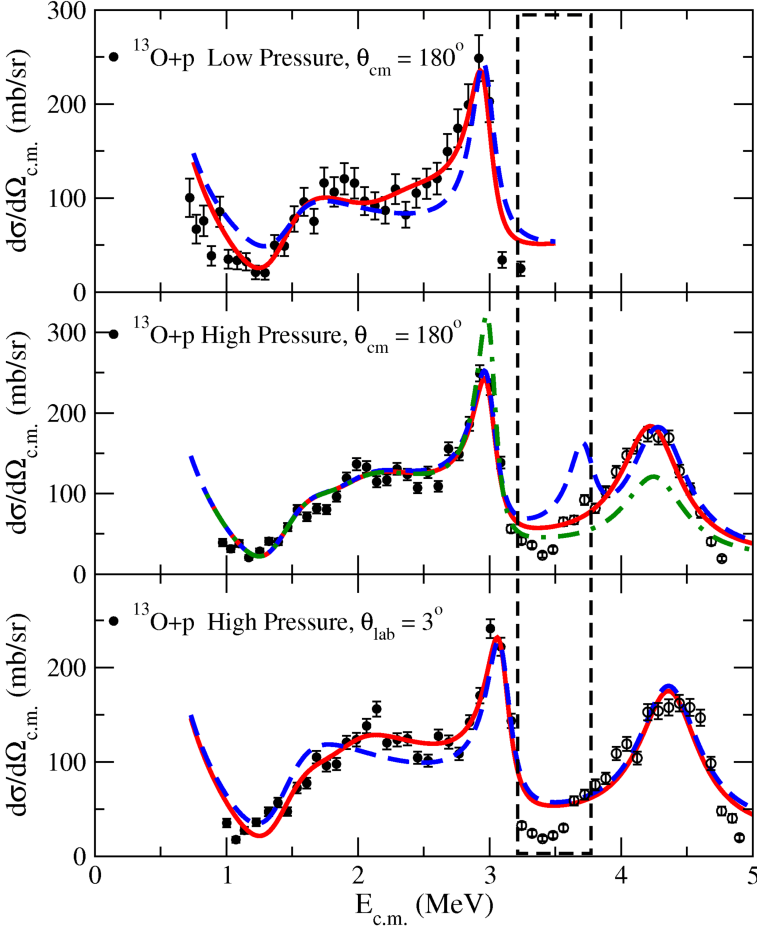


Fig. 2. Excitation functions for $^{13}\text{O} + p$ elastic scattering are given with R-matrix calculations. The solid line (red) is the best fit calculation using the ^{14}F level scheme as given in Table I. The dashed box shows the region of distorted data because the QSD detector was not fully depleted. Top panel: The dashed line (blue) is a fit with 1^- as the ground state. Middle panel: The dashed line (blue) is a calculation with a second hypothetical 2^- state at higher excitation energy. The dash-dotted line (green) is a calculation with a 4^- state at 3 MeV (instead of 3^-) and a 3^- state at 4.35 MeV (instead of 4^-). Bottom panel: The dashed line (blue) is the fit without the 1^- first excited state.

which were obtained using the exotic beam with unusually low intensity and a large energy spread. According to the R-matrix fit, the ground state in ^{14}F is definitely 2^- . Only $\ell = 0$ resonances are simultaneously broad enough and provide for the needed interference with the Coulomb amplitude.

A 1^- resonance as the ground state would be too weak to provide for the deep minimum in the excitation function (dashed line in the top panel of Fig. 2). However, a 1^- state is expected to be the first excited state in the *ab initio* calculations [9] (see Fig. 3).

TABLE I

 Levels in ^{14}F .

E_R [MeV] [†]	E_x^*	J^π	Γ [keV]	$\Gamma/\Gamma_{\text{sp}}$
1.56 ± 0.04	0.00	2^-	910 ± 100	0.85
2.1 ± 0.17	0.54	1^-	~ 1000	0.6
3.05 ± 0.060	1.49	3^-	210 ± 40	0.55
4.35 ± 0.10	2.79	4^-	550 ± 100	0.5

[†]Energy above $^{13}\text{O} + p$ decay threshold.

*Excitation energy in ^{14}F .

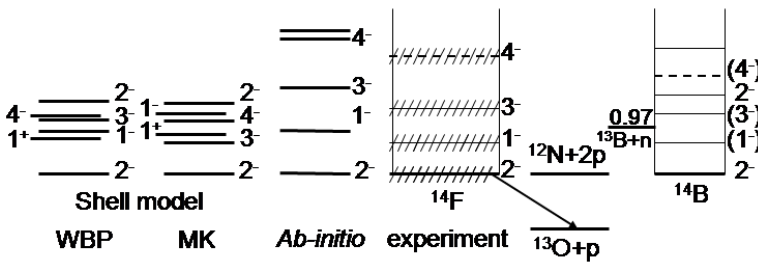


Fig. 3. ^{14}F level scheme compared with shell-model calculations, *ab initio* calculations [9] and the ^{14}B level scheme [13]. The shell model calculations were performed with the WBP [18] and MK [19] residual interactions using code COSMO [20].

The inclusion of a broad 1^- resonance improved the fit by 40%, though its presence is not obvious in an inspection by eye (bottom panel in Fig. 2). Any resonance with $\ell > 0$ would produce a narrow peak in the region of the 1^- resonance, and should be excluded. The peaks at 3 MeV and 4.3 MeV were fit by *d*-wave resonances with large reduced widths and with spins 3^- and 4^- respectively (see Table I). As seen in Table I, ^{14}F is unstable by 1.56 MeV relative to proton decay, which corresponds to an atomic mass excess of 31.96 ± 0.05 MeV using the mass tables in [10]. In [11], ^{14}F was predicted to be unstable by ~ 3 MeV based on the systematics of masses of light nuclei. Then, it was extrapolated to be unbound by 2.26–2.58 MeV in [10, 12, 13]. The recent *ab initio* calculations [9] also predicted it to be unbound by ~ 3 MeV. While new calculations are needed to specify the necessary corrections to the theoretical approaches, part of the disagreement between the predictions and the present result should be related with

the Thomas–Ehrman shift [14, 15] of levels in mirror nuclei. This energy shift down toward greater stability in proton rich nuclei is the largest (and therefore famous) for s -states. A small part of this shift is related with the change of boundary conditions (due to change in the binding energy), and the rest is due to the possibility to find the proton with orbital momentum $\ell = 0$, far from the core, in a lower Coulomb field [16]. Hence, the shift is strongly dependent upon the single particle structure of the state. As reported in Table I, the ground state in ^{14}F has nearly pure single particle structure and we can estimate the effect of the Thomas–Ehrman shift on the ^{14}F binding energy. Assuming the ground states in the mirror nuclei ^{14}B and ^{14}F have the same structure and using the potential parameters which have been found for ^{15}F in [17], we fit the binding energy of ^{14}B relative to the neutron decay threshold (0.97 MeV). The depth of the potential well was found to be 54.485 MeV. Then, using these parameters, we calculated that ^{14}F should be unbound to proton decay by 1.45 MeV. This number differs by only 0.11 MeV from the experimental value of 1.56 MeV. However, if we assume that the ground state in ^{14}B (^{14}F) is a d -state (or a state of complicated nature), a similar procedure will result in ^{14}F being unbound by 2.35 MeV, which is much closer to all theoretical estimates. Thus, the main part ($2.35 - 1.45 = 0.9$ MeV) of the unexpected stability of ^{14}F can be ascribed to a purity of the $2s$ state configuration of the ground state.

It is easy to note looking at Fig. 3 that the shell model calculations produce a much more compressed level scheme than the *ab initio* calculations. The latter are in better agreement with the experimental data. We suppose that this indicates that the residual interactions should be modified in the shell model for a better description of exotic nuclei.

3. Missing resonances in ^8B

The neutron deficient Boron isotope, ^8B , has proton separation energy of only 137 keV and all of its excited states are in the continuum. This nucleus has been a subject of numerous theoretical studies. The low lying positive parity states (0^+ , 2^+ , 1^+) were predicted [21, 22] but never observed experimentally (except for the 1^+ at 3.0 MeV suggested in [23]). In the recent *ab initio* NCSM/RGM analysis [24] of ^8B , the $p + ^7\text{Be}$ elastic scattering phase shifts as well as the cross section for the $^7\text{Be}(p, p')$ and the $^7\text{Be}(p, \gamma)$ reactions were calculated. Search for the “missing” resonances in the $^7\text{Be} + p$ resonance scattering and direct comparison of the experimental results on the $^7\text{Be}(p, p)$ and $^7\text{Be}(p, p')$ reactions with the *ab initio* calculations is discussed below.

The excitation functions for $p + ^7\text{Be}$ elastic and inelastic scattering between 1.6 and 3.4 MeV in c.m.s. were measured at the John D. Fox Superconducting Accelerator Laboratory at Florida State University. Experimental details and details of the R-matrix analysis are discussed in [6].

The excitation functions for elastic ${}^1\text{H}({}^7\text{Be}, p){}^7\text{Be}(\text{g.s.})$ and inelastic ${}^1\text{H}({}^7\text{Be}, p'){}^7\text{Be}(1/2^-; 0.43 \text{ MeV})$ are shown in Fig. 4. The three known states [25], the 1^+ at 0.77 MeV, the 3^+ at 2.32 MeV and the broad 2^- at ~ 3 MeV reproduce the excitation function for $p+{}^7\text{Be}$ elastic scattering between 0.5 and 3.5 MeV reasonably well. However, it is not possible to explain 30 mb/sr inelastic cross section at 2.5 MeV if only known states in ${}^8\text{B}$ are considered. Based on the level scheme of ${}^8\text{Li}$, we introduce the second 1^+ state in ${}^8\text{B}$ at an excitation energy around 3 MeV. While the elastic excitation function is fitted well, the inelastic cross section is still underestimated.

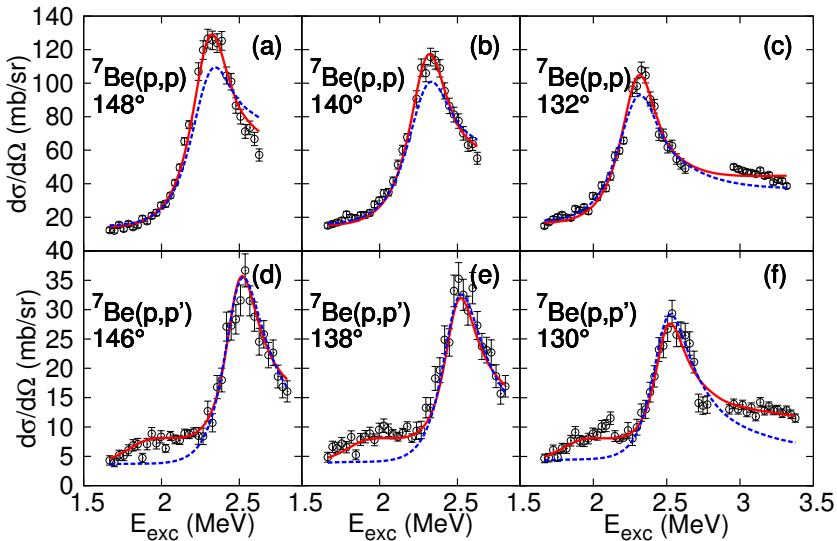


Fig. 4. Elastic and inelastic excitation functions for ${}^7\text{Be} + p$ scattering. The dashed/blue curve is a fit with the previously known 1^+ and 3^+ states as well as a 2^- at 2.54 MeV to reproduce the peak in the inelastic data. The 2^- and 1^- phase shifts were varied. The solid/red curve is the best R-matrix fit with the previously known states and also with the 0^+ at 1.9 MeV and 2^+ at 2.54 MeV.

The *ab initio* calculations for ${}^8\text{B}$ [1, 2, 24] predict three more positive parity (p -shell) states at low excitation energy. These are the 0^+_{1} , 1^+_{2} and 2^+_{2} . The excitation energies for these states vary between 2 and 6 MeV depending on the three-body force parameterization and the specifics of the calculations. Therefore, it is natural to introduce these states in an attempt to reproduce the large inelastic scattering cross section. Introduction of a new 2^+ state placed at 2.5 MeV reproduces both the magnitude and angular dependence of the observed peak in the inelastic cross section while keeping the elastic excitation function in agreement with the experimental data (dashed/blue curve in Fig. 4). However, even with this new state, the

cross section for inelastic scattering below 2.3 MeV is still underestimated. The 2^+ state should have a relatively small width (270 ± 40 keV) to fit the observed peak-like structure in the inelastic excitation function at 2.5 MeV and its influence below 2.3 MeV is small. Introducing the 0^+ state at an excitation energy of 1.9 ± 0.1 MeV with a width of 530_{-100}^{+600} keV allows the inelastic scattering data to be fit below 2.3 MeV without destroying the fit to the elastic scattering data (solid/red line in Fig. 4). Therefore, this data provides the first direct evidence of the “missing” low lying excited states in ^8B .

With the development of the *ab initio* NCSM/RGM approach [24], the *ab initio* phase shifts can now be compared directly to the experimental phase shifts extracted from the R-matrix analysis of the experimental data. The $^7\text{Be} + p$ diagonal phase shifts as well as $^7\text{Be}(p, p')$ excitation function have been calculated in Ref. [3].

The shape of the 3^+ diagonal phase shift is determined by the 3^+ state at 2.29 MeV, which only has contribution from channel spin $S = 2$ and no inelastic component. NCSM/RGM overestimates the excitation energy of this state by ~ 1 MeV, otherwise the phase shift is similar to the experimental one.

Comparison of the 1^+ phase shifts from the best fit and from the [3] is shown in Fig. 5. The phase shifts appear to be very dissimilar. The 1_1^+ state shows up predominantly in the $S = 1$ channel in the best fit and it is located at lower energy than predicted in [3]. This makes the contribution from the inelastic channel negligible and the $S = 1$ phase shift goes through

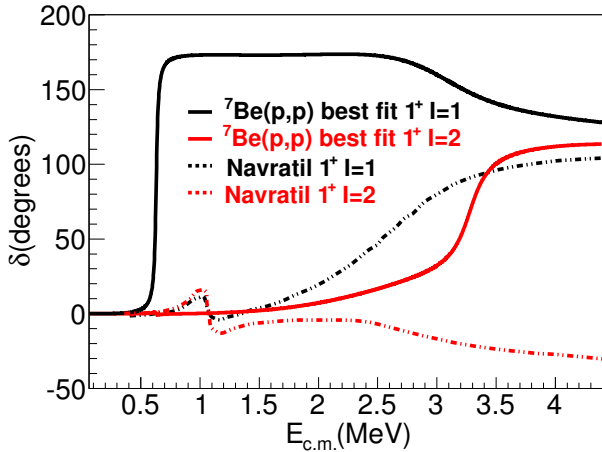


Fig. 5. The 1^+ phase shifts from the best fit and from [3]. Best fit R-matrix phase shifts for channel spins 1 and 2 are black and gray/red solid curves respectively. The dash-dotted black and gray/red curves are $S = 1$ and $S = 2$ 1^+ phase shifts from [3].

90 degrees, unlike in [3]. A more important difference is that the best fit $S = 2$ phase shift barely shows any sign of the 1_1^+ state, while the *ab initio* $S = 2$ and $S = 1$ phase shifts have about equal contributions from the 1_1^+ state. However, another good fit with comparable (although slightly worse) χ^2 can be achieved with the phase shifts similar to those calculated in Ref. [3, 24].

The 1_2^+ state is responsible for the behavior of the 1^+ phase shifts above 1 MeV. Comparing the best fit and *ab initio* phase shifts, one can notice that at higher energies the best fit $S = 1$ phase shift is similar to the $S = 2$ *ab initio* phase shift, and the best fit $S = 2$ phase shift is similar to the $S = 1$ *ab initio* phase shift. We have produced another fit using the *ab initio* 1^+ phase shifts from [3] and varied parameters for all other states. This fit has a χ^2 of 1.2. The fit to the inelastic data is visually identical. The quality of the fit to the elastic scattering data is somewhat worse. Observable parameters for all other positive parity states were still within the uncertainties quoted in Table II. Generally, while the best fit 1^+ phase shifts look very different, we find that the data can be reproduced reasonably well with the 1^+ phase shifts from [3]. This ambiguity can be resolved if a wide range of angles and energies are measured with high accuracy and/or experiment is performed with a polarized target.

TABLE II

Parameters of resonances in ^8B from the R-matrix best fit.

J^π	E_{ex} [MeV]	Γ_{tot} [MeV]	Γ_p [MeV]	$\Gamma_{p'}$ [MeV]
1^+	0.768(4)	0.027(6)	0.026(6)	0.001
0^+	1.9(1)	$0.53^{+0.6}_{-0.1}$	$0.06^{+0.3}_{-0.02}$	$0.47^{+0.4}_{-0.1}$
3^+	2.31(2)	0.33(3)	0.33(3)	0.0
2^+	2.50(4)	0.27(4)	0.05	0.22
1^+	3.3(2)	3.2(9)	2.8	0.4

The 0^+ phase shift is defined by the 0^+ resonance at 1.9 MeV. Figure 6 shows the 0^+ phase shifts from the best fit and the *ab initio* calculations [3]. The two phase shifts are very similar, indicating that the structure of the 0^+ state is well reproduced in [3]. In order to have a perfect match between our phase shift and that from [3], it is necessary to increase the total width of the state to ~ 1 MeV. A fit to the experimental data with the 0^+ phase shift from [3] produces a χ^2 value of 0.97 and is almost indistinguishable visually. This is because the stronger 0^+ is compensated by the modifications to the negative parity phase shifts and the parameters for the other positive parity states remain almost unchanged. This is why the 0^+ state has a large uncertainty for its widths (see Table II).

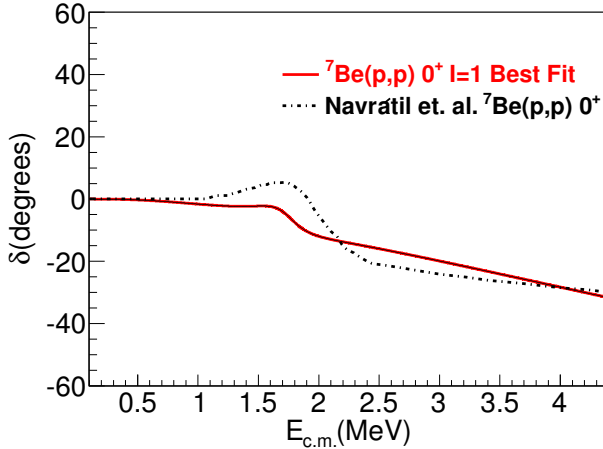


Fig. 6. The 0^+ phase shifts from the best fit (solid/red curve) and from [3] (dash-dotted/black curve).

The only obvious difference between the experimental data and the results of NCSM/RGM calculations [24] is related to the 2^+ phase shift. The 2_2^+ state is predicted at 4 MeV by the NCSM/RGM calculations. The channel spin 2 diagonal phase shift goes through 90° and the spin 1 phase shift becomes negative at the resonance [24]. The R-matrix best fit to the observed 2_2^+ state produces similar behavior for the channel spin 1 diagonal phase shift near the resonance but the spin 2 phase shift does not go through

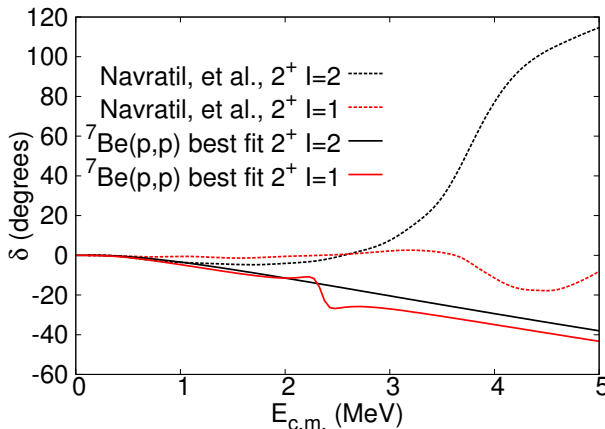


Fig. 7. Comparison of the experimental best fit 2^+ phase shifts to the calculated phase shifts of [24]. R-matrix calculations for channel spins 2 and 1 are solid (black and gray/red) curves respectively, while those of [24] are dashed (black and gray/red) curves respectively.

90° and does not show any sign of the 2_2^+ resonance at all. The dominant decay mode for the experimental 2_2^+ state is into the first excited state of ${}^7\text{Be}(1/2^-)$. This produces the characteristic shape of the channel spin 1 2^+ phase shift, but the channel spin 2 reduced width amplitude is zero and the corresponding phase shift does not show the 2_2^+ state. This is shown in Fig. 7. It appears that the 2^+ state predicted in Ref. [3, 24] and the observed 2^+ are two different states. We can speculate that the situation here may be similar to the predictions of the conventional shell model CKI Hamiltonian, that produces two 2^+ states at 4.2 and 5.1 MeV, and only the latter has the correct structure. It is possible that the lowest 2^+ state predicted by the NCSM/RGM calculations is not the one observed in this experiment.

4. Conclusion

As our test shows, *ab initio* calculations have become an important practical tool for predictions in nuclear structure and reactions. This approach still contains “free” parameters which are a result of insufficient knowledge of details of the N - N interaction or of many body forces. Evidently, these parameters have more fundamental meaning than in other phenomenological approaches. The best test of these parameters is provided by properties of light nuclei away from the valley of stability because of their unusual N/Z ratio and because low lying states are unstable to nucleon decay so that *ab initio* approaches and resonance reactions induced by rare beams complement each other.

REFERENCES

- [1] P. Navratil *et al.*, *Phys. Rev.* **C57**, 3119 (1998).
- [2] R. Wiringa *et al.*, *Phys. Rev.* **C62**, 014001 (2000).
- [3] P. Navratil *et al.*, *Phys. Rev.* **C82**, 034609 (2010).
- [4] V.Z. Goldberg *et al.*, *Phys. Lett.* **B692**, 307 (2010).
- [5] J.P. Mitchell *et al.*, *Phys. Rev.* **C82**, 011601(R) (2010).
- [6] J.P. Mitchell *et al.*, *Phys. Rev.* **C87**, 054617 (2013).
- [7] R.E. Tribble *et al.*, *Nucl. Instrum. Methods* **A285**, 441 (1989).
- [8] K.P. Artemov *et al.*, *Sov. J. Nucl. Phys.* **52**, 406 (1990).
- [9] P. Maris *et al.*, *Phys. Rev.* **C81**, 021301(R) (2010).
- [10] G. Audi *et al.*, *Nucl. Phys.* **A729**, 337 (2003).
- [11] G.C. Ball *et al.*, *Phys. Rev. Lett.* **31**, 395 (1973).
- [12] M.S. Antony *et al.*, *At. Data Nucl. Data Tables* **34**, 279 (1986).
- [13] F. Ajzenberg-Selove, *Nucl. Phys.* **A523**, 1 (1991).

- [14] R.G. Thomas, *Phys. Rev.* **81**, 148 (1951).
- [15] J.B. Ehrman, *Phys. Rev.* **81**, 412 (1951).
- [16] A. Nolen, J.P. Schiffer, *Annu. Rev. Nucl. Sci.* **19**, 471 (1969).
- [17] V.Z. Goldberg *et al.*, *Phys. Rev.* **C69**, 031302(R) (2004).
- [18] E.K. Warburton, B.A. Brown, *Phys. Rev.* **C46**, 923 (1992).
- [19] D.J. Millener, D. Kurath, *Nucl. Phys.* **A255**, 315 (1975).
- [20] A. Volya, *Phys. Rev.* **C79**, 044308 (2009).
- [21] P. Navratil *et al.*, *Phys. Rev.* **C73**, 065801 (2006).
- [22] S.C. Pieper *et al.*, *Phys. Rev.* **C70**, 054325 (2004).
- [23] V.Z. Goldberg *et al.*, *JETP Lett.* **67**, 1013 (1998).
- [24] P. Navratil *et al.*, *Phys. Lett.* **B704**, 379 (2011).
- [25] D.R. Tilley *et al.*, *Nucl. Phys.* **A745**, 155 (2004).